CURCUMIN AND WHEY PROTEIN BINDING AND STRUCTURAL CHARACTERISTICS OF THEIR COMPLEX EVIDENCED BY ATOMIC FORCE MICROSCOPY

LEVENTE ZSOLT RACZ[a], GERTRUD-ALEXANDRA PALTINEAN[a], IOAN PETEAN[a], GHEORGHE TOMOAIA[b,c] , LUCIAN CRISTIAN POP[a], GEORGE ARGHIR[d], ERIKA LEVEI[e], AURORA MOCANU[a], CSABA-PAL RACZ[a], MARIA TOMOAIA-COTISEL[a,c] *

ABSTRACT. Curcumin (CCM) has beneficial effects on human health due to its pharmacological activities, which have a protective role against many diseases. Whey protein concentrate (WPC) is a product from the milk industry that is often used to improve and stabilize different foods. It helps curcumin improve its water solubility, poor bioavailability, low stability, and efficacy. Atomic force microscopy (AFM) was employed to highlight the surface topography of adsorbed films of pure curcumin, pure whey protein concentrate, and their CCM-WPC complex. The obtained results show that individual nanoparticles, NPs, were mobilized into the aqueous dispersion and successfully adsorbed onto the glass slides as thin films. Their NPs shape is rounded, and their diameter differs on each sample, namely about 30 nm for CCM, around 55 nm for WPC, and about 40 nm for the CCM-WPC complex. It proves that both CCM and WPC molecules generate a complex that embeds them in a compact structure. The surface roughness was also monitored, and pure CCM produces the smoothest and uniform film, meanwhile, the presence of WPC makes several pores in the film surface which increases the roughness value. The obtained results provide useful evidence for the application of whey protein as an effective carrier of curcumin, a bioactive polyphenol compound. In addition, this work supports the application of the CCM-WPC complex as health supplements.

Keywords: *Curcumin, whey protein concentrate, curcumin-whey protein complex, AFM, nanostructure, roughness*

[a] *Babeş-Bolyai University, Research Center of Physical Chemistry, Faculty of Chemistry and Chemical Engineering, 11 Arany Janos str., RO-400028, Cluj-Napoca, Romania*
[b] *Iuliu Hatieganu University of Medicine and Pharmacy, Department of Orthopedics and Traumatology, 47 Gen. Traian Mosoiu str., RO-400132, Cluj-Napoca, Romania*
[c] *Academy of Romanian Scientists, 3 Ilfov str., RO-050044, Bucharest, Romania*
[d] *Technical University, Faculty of Materials and Environment Engineering, 103-105 Muncii Boulevard, RO-400641, Cluj-Napoca, Romania*
[e] *INCDO-INOE2000, Research Institute for Analytical Instrumentation, 67 Donath str., RO-400293 Cluj-Napoca, Romania*
* *Corresponding author: mcotisel@gmail.com*

L. ZS. RACZ, G.-A. PALTINEAN, I. PETEAN, GH. TOMOAIA, L. C. POP, G. ARGHIR,
E. LEVEI, A. MOCANU, C.-P. RACZ, M. TOMOAIA-COTISEL

INTRODUCTION

Curcumin (CCM) is a nutraceutical substance with many pharmacological activities such as antioxidant, anticancer and analgesic, anti-inflammatory, antiseptic, antiviral, antidiabetic, and antiparasitic, for which researchers' attention was directed to its study in the biomedical field [1]. This aspect is well documented in the literature: CCM prevents inflammatory diseases, inhibits carcinogenesis, controls neurological, respiratory, cardiovascular, metabolic, autoimmune diseases, and some cancers [2, 3]. It is a small molecular weight compound extracted from the rhizomes of the *Curcuma longa* plant and is used as a yellow spice in the food industry. Specialized literature and the Food and Drug Administration declared that curcumin utilization is safe and without toxic effect [4]. It is known as diferuloylmethane or (1E,6E)-1,7-bis(4-hydroxy-3-methoxyphenyl)-hepta1,6-diene-3,5-dione). Its structure contains two aromatic rings having phenolic o-methoxy groups, connected by a β-diketone fragment.

Curcumin has low water solubility that contributed to its poor bioavailability, stability, adsorption, and efficacy, limiting its therapeutic potential [5-9]. Approaches to improving this limitation of curcumin properties were highlighted in some research studies by the preparation of complex systems between curcumin and phospholipids, curcumin and proteins (whey protein, pea proteins, soy proteins or rice bran proteins), curcumin and β-cyclodextrins (βCD), and other colloidal systems for encapsulation or drug delivery based on liposomes, micelles and polymers [10-12]. CCM binds to proteins molecules through hydrogen bonds forming a complex that can improve the dispersibility, bioavailability and biological activity of curcumin [13]. β-Lactoglobulin is the main component of the whey protein which has the capacity to bind to CCM due to its hydrophobic core and its resistance to pepsin digestion. Therefore, the complex made by β-lactoglobulin and CCM can be an effective carrier of CCM in the intestinal tract to treat inflammatory bowel disease [14, 15]. In the case of cyclodextrins, the dedicated literature reveals that cyclodextrins are the best carriers for enhancing the solubility of CCM. The conical cavities of cyclodextrins are able of including various organic guests and form inclusion complexes. Regarding the CCM-βCD inclusion complexes, the literature emphasizes the release of drug and drug stability [16-20].

Whey protein concentrated (WPC) is a product resulting from cheese manufacturing in the milk industry. Whey protein is used as an ingredient in foods such as dairy, bakery products, beverages, and meat products [21]. It is a low-cost chemical product that is non-toxic and presents good biocompatibility. WPC is a mixture of β-lactoglobulin (57%), α-lactalbumin

(19%), immunoglobulins which are actually some glycoprotein molecules (13%), bovine serum albumin (7%) and specific polypeptides (4%), additional minor protein/peptide components (lactoferrin, lactoperoxidase), glycomacropeptide, carbohydrates such as lactose, minerals, vitamins, fatty acids, and cholesterol (a lipid) [22-25]. The data in the literature highlighted that the whey protein possesses some functional attributes which allowed the encapsulation of molecules such as curcumin, to improve the solubility and bioavailability. In addition, it can form gels, foams, or emulsions when is used in food products [26]. Whey proteins are in 3 forms on the market: concentrates, isolates, and hydrolysates. The difference between them is given by the percentage of protein; the concentrate has fat, lactose, and proteins 29-89%, the isolate 90 % proteins and the hydrolysates represent the partial digested type of proteins. All these forms of whey proteins have some biological activity such as anticancer, antioxidant, antidiabetic, antihypertensive [6, 23, 27, 28].

The benefits of the CCM-WPC complex are highlighted in the literature as: high resistance under gastric conditions; antitumor effects against skin melanoma cells and its ability to decrease blood glucose and liver oxidative stress and inflammatory damage [6, 28, 29]. Some studies use nano-ionization to fabricate curcumin-whey protein composite particles and show that denaturation of whey protein improves the protein-curcumin interactions [30].

According to the fact that whey proteins, such as β-lactoglobulin, have internal and external binding sites for hydrophobic molecules, such as curcumin, and varied interactions, such as hydrophobic and electrostatic interactions, as well as hydrogen bonding can occur between these proteins and curcumin.

The curcumin-whey protein complex in the 1:1 mole ratio was previously investigated by FTIR and XRD, and the encapsulation of CCM in the WPC was revealed [6].

In the present research, our aim was to gain an understanding of the binding between curcumin and whey protein concentrate nanoparticles using the AFM images. To the best of our knowledge, this is the first study with whey protein concentrate as a nano-carrier and curcumin under physiological condition. This investigation could be of support for the stabilization and delivery of curcumin under different environmental conditions to increase its bioavailability and biological effects.

L. ZS. RACZ, G.-A. PALTINEAN, I. PETEAN, GH. TOMOAIA, L. C. POP, G. ARGHIR,
E. LEVEI, A. MOCANU, C.-P. RACZ, M. TOMOAIA-COTISEL

RESULTS AND DISCUSSION

AFM is a useful technology for the characterization of the materials microstructure, nanostructure, and nanomechanical properties [31]. It represents multidisciplinary research in the field of bio nanostructures [32-34], thin films [35, 36], multifunctional biomaterials [37-43], and environmental pollution [44, 45]. AFM is a complex investigation method that allows: measuring surface roughness and characteristics of samples [46-54], analyzing the interaction of the cell membrane with drugs [55-59]. Also, it is useful to visualize the self-assemblies of biomolecules and allows measuring the average particles diameter [60].

AFM may be operated in three modes: contact mode, non-contact, and tapping mode. In this research we use AFM in tapping mode to evaluate the surface morphology and roughness of the samples.

The curcumin powder dispersed in ultrapure water ensures a mobilization of nanoparticles that are in Brownian agitation. Glass slide immersion into the curcumin dispersion for 10 seconds facilitates these nanoparticles to reach the lamella surface and to be adsorbed on it. They remain well fixed, ensuring a very well-formed film after natural drying, as observed from the macroscopic examination of the sample. AFM imaging allows us to observe the nanostructure of this thin film, Figure 1.

The topography of the surface reveals curcumin nanoparticles with spherical shape uniformly adsorbed ensuring a good cohesion of the film, Figure 1a. They are adsorbed in a uniform manner avoiding sticking. This aspect is due to the low solubility of curcumin in aqueous medium. Therefore, the nanoparticles remain sharp and keep their diameter unchanged in contact with water. At the same time, these nanoparticles are very well individualized, appearing well outlined in the phase image, Figure 1b, where they have a brown nuance, and the space between them (the boundary between them) appears with a yellow colour. This is due to the well-defined nanoparticle boundaries. The amplitude image sustains the good structuring of the adsorbed film, Figure 1c, evidencing the uniformity of the adsorbed nanoparticles layer. The profiles in the topographic image show the rounded appearance of the nanoparticles and their diameter around 30 nm, fact confirmed by the particle size distribution histogram in Figure 1f. The regularity of the film leads to very low values of surface roughness expressed as the quadratic mean of the profile height deviations as root mean square, RMS of about 4.76 nm, and arithmetic average roughness, Ra nearby 3.82 nm. The obtained values are comparable to the ones for similar thin films reported in the literature [35, 36].
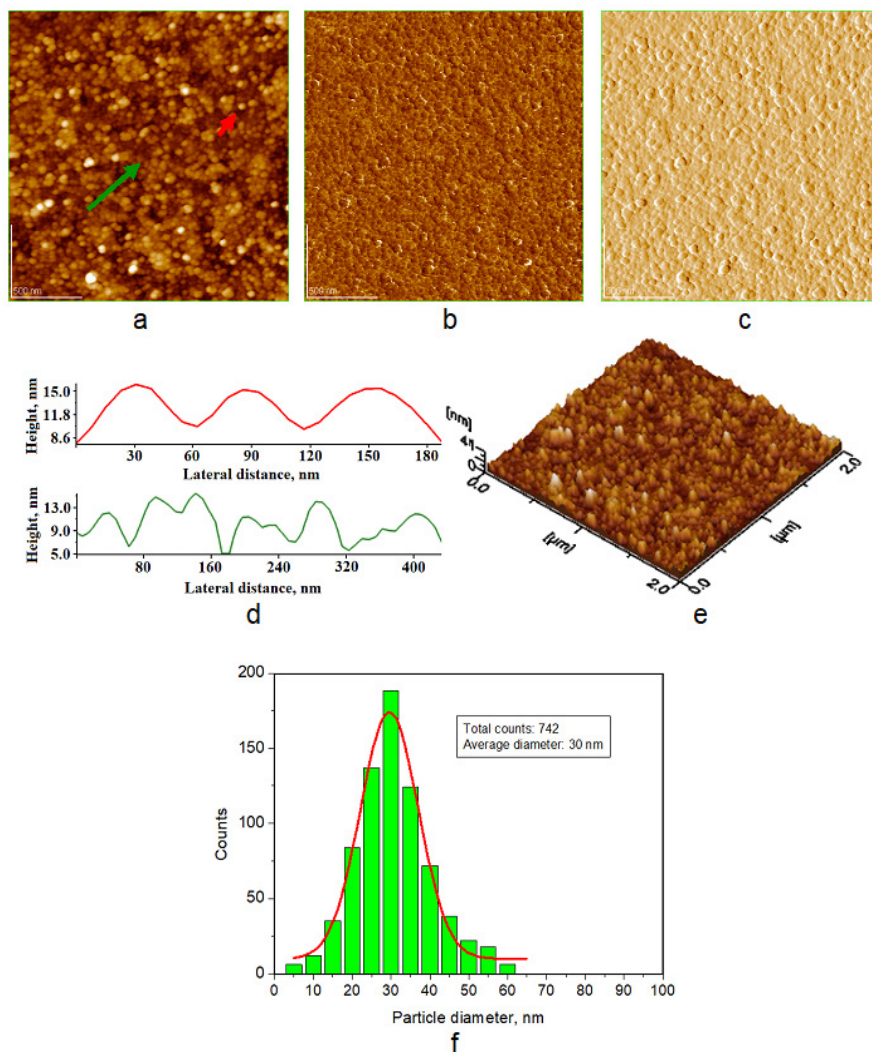
Figure 1. AFM images of CCM NPs adsorbed on glass and naturally dried:
a) topographic image, b) phase image, c) amplitude image, d) profiles along
the arrows in panel (a), e) tridimensional image and f) histogram
of particle size distribution. Scanned area 2 µm x 2 µm.

A prolonged adsorption time could lead to the WPC nanoparticles dissolution due to their particular water solubility. The adsorption time control is one of the most important parameters when working with whey protein.

The whey protein concentrate was successfully dispersed in an aqueous environment, ensuring optimal conditions for the transfer of nanoparticles on the glass support by adsorption for 10 seconds, Figure 2.
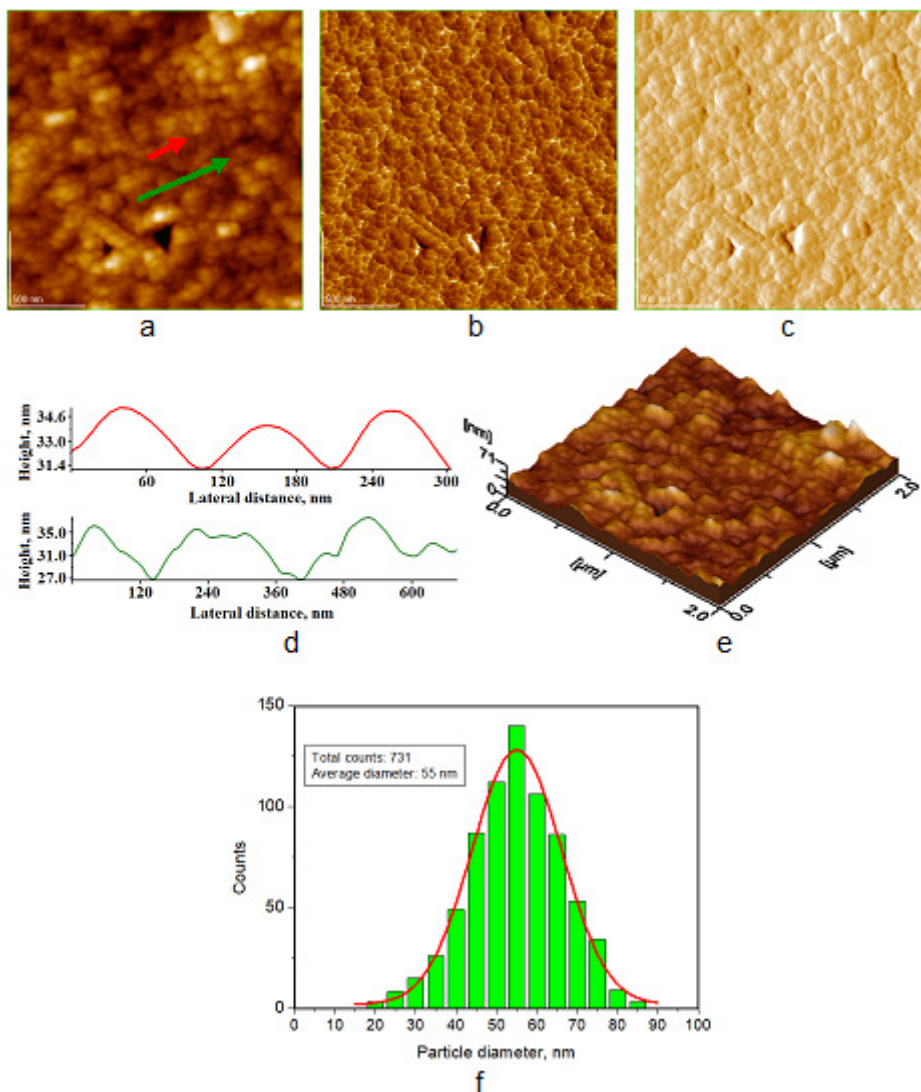

Figure 2. AFM images of WPC NPs adsorbed on glass and naturally dried: a) topographic image, b) phase image, c) amplitude image, d) profiles along the arrows in panel (a), e) tridimensional image and f) histogram of particle size distribution. Scanned area 2 µm x 2 µm.

The topography of the obtained film highlights a uniform adsorption of the nanoparticles. They present a rounded shape and a high agglomeration tendency being adsorbed very close to each other. The revealed topographical aspect in Figure 2a confirms the success of adsorption. On the other hand, the agglomeration tendency is explained by the partial solubility of WPC in aqueous environment. The nanoparticles surface become sticky in such humid conditions and tends to bond them together, forming clusters. Several pores were observed in some places with diameters between 60 and 180 nm as well as a slight tendency to form clusters as can be seen in the upper right corner of the image. Cluster formation is inhibited by the short adsorption time and the dilution in the dispersion; Figure 2a. However, most of the film areas are uniform and show a good individualization of the nanoparticles, although they are very close to each other. This is supported by the phase image, Figure 2b, where the boundary between the nanoparticles is very small and appears yellow, while the nanoparticles are brown. The tendency to form clusters is, however, very weak because they cannot be observed in the amplitude image, Figure 2c, but instead, in this image one can see the porosity of the sample. This leads to a roughness RMS of around 6.53 nm and Ra of about 5.09 nm. These aspects are perfectly correlated with the 3D topographic image in Figure 2e. The cross-section profiles of the topographic image highlight the rounded shape of the nanoparticles and indicate their average diameter around 55 nm. This is in full agreement with the data from the particle size distribution histogram, Figure 2f. It seems that the partial solubility on WPC nanoparticles in aqueous environment determined the appearance of the pores in the adsorbed film topography.

Complexation between curcumin and whey protein concentrate shows significant changes in the morphology and behaviour of the resulting powder. Its dispersion in ultrapure water releases nanoparticles that are adsorbed in a uniform way on the glass surface. AFM images prove to be strong evidence of this effect, Figure 3.

The surface topography shows a thin film of round nanoparticles uniformly adsorbed on the glass slide. The resulted morphology is complex containing elements from both components: from curcumin is observed the good individualization of the nanoparticles and from whey protein the tendency for pore formation is observed (pore size situated in the range of in 60 to 90 nm). The nanoparticles were adsorbed very close to each other, but they are not bonded together, keeping their individuality, fact very well evidenced by the phase and amplitude image, Figures 3b and 3c.

The appearance of the 3D image is smooth and uniform, but the significant presence of pores determines the roughness values of RMS about 6.62 nm and Ra nearby 5.00 nm. The cross-section profiles in Figure 3d show the nanoparticles rounded shape and the average diameter of 40 nm, fact in accordance with the particle size distribution in Figure 3f. Data in the

literature indicates diameters of WPC nanoparticles of about 40 nm [61, 62]. The pores presence in the CCM-WPC thin film is collateral evidence of complex solubility increasing. Pore development within the tin film may occur due to the local dissolution of some WPC nanoparticles in the contact with humid environment.
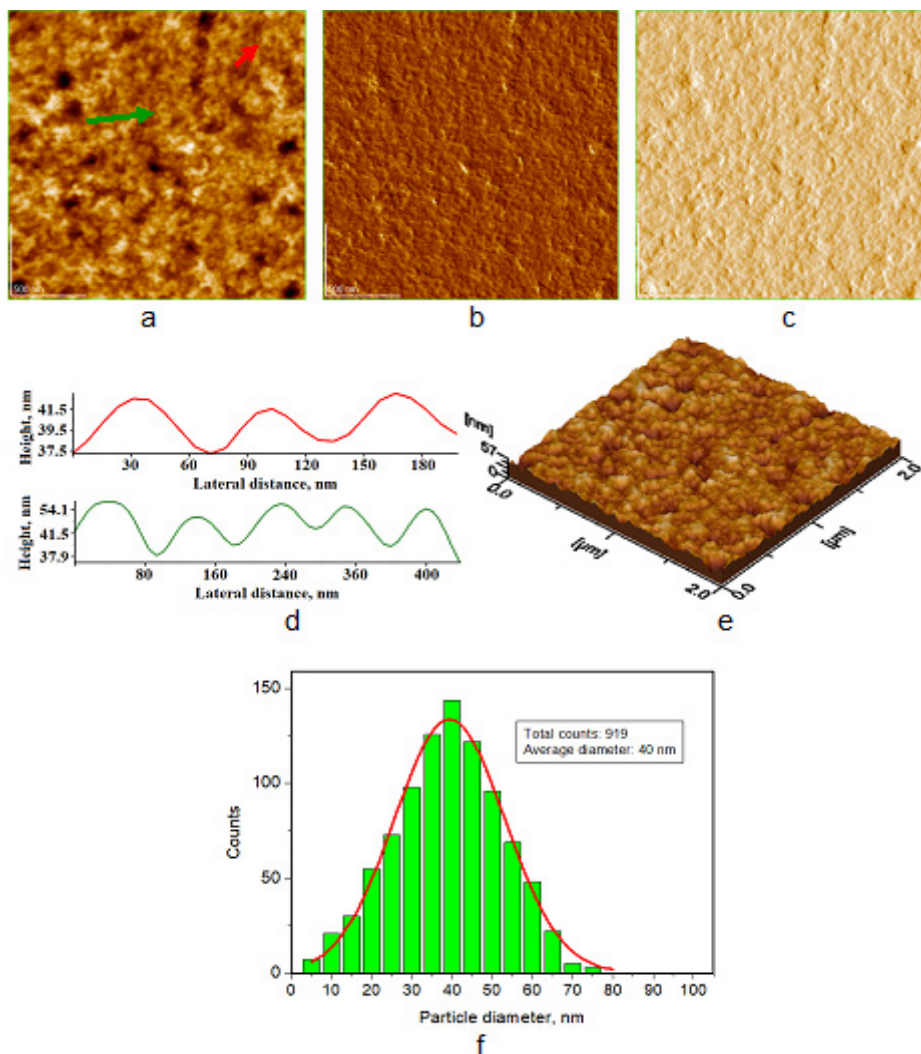

Figure 3. AFM images of the CCM-WPC complex, obtained at pH 7.4, adsorbed on glass and naturally dried: a) topographic image, b) phase image, c) amplitude image, d) profile along the arrow in panel (a), e) tridimensional image and f) histogram of particle size distribution. Scanned area 2 μm x 2 μm.

The nanostructure evolution in the CCM – WPC system reveals that the complex nanoparticles have a larger diameter than that of pure curcumin, but smaller than that of concentrated whey protein. This is a proof of the interpenetration of the CCM and WPC, in good agreement with the microscopically observation in the literature [61]. Therefore, the initial state of the CCM-WPC complex is a dry powder just like many other dietary supplements on the market. The present research evidences the CCM-WPC ability to release nanoparticles into the aqueous environment that is similar to the one release in the stomach medium. AFM investigation sustains the CCM-WPC nanoparticles affinity to be adsorbed on the surfaces. It may be a useful behavior during digestion to enhance contact with the small intestine walls.

The observations within present research allow us to figure out two ways of CCM-WPC delivery into the gastric system: the direct one using a classic dissolvable capsule with complex powder at the proper dosage or a pressed pill; and the indirect delivery which is supposed to encapsulate the complex powder into a microsphere. The CCM-WPC powder encapsulation in a microsphere made of dissolvable material presents the benefit of controlled release during digestion, avoiding premature contact of the nanoparticles with the digestive juice and the intestine wall. These aspects represent a challenge for the future.

CONCLUSIONS

The nanostructures of the CCM-WPC system were successfully investigated by atomic force microscopy which is a fundamental method for the nano characterization of materials. Both initial CCM and WPC powders were able to form nanoparticles into aqueous environment. These nanoparticles were adsorbed onto a glass substrate, forming thin films. Their shape is rounded, and their diameter differs on each sample: about 30 nm for CCM, around 55 nm for WPC.

The complexation involved between CCM and WPC leads to an intermediary diameter of approximately 40 nm. CCM nanoparticles are uniformly adsorbed on the glass surface, generating a smooth film with low roughness. WPC tends to generate pores on the adsorbed film, which leads to relatively higher values of the roughness. The CCM-WPC complex forms a smooth thin film, but the influence of WPC within the composition still generates some pores that affect the roughness value.

These results might support the development of functional foods including curcumin and whey protein, with new uses in yoghourt and nutritional supplements.

EXPERIMENTAL SECTION

Materials

Curcumin from *Curcuma longa* powder ≥ 65%, ethanol (CH_3CH_2OH) 95%, were purchased from Sigma-Aldrich, Darmstadt, Germany; Whey protein concentrate (WPC) contains about 80% protein and it was purchased from Foodcom S.A. Warsaw, Poland. Ammonia solution 25% was purchased from Merck, Darmstadt, Germany. Ultrapure water (resistivity of 18.2 MΩ x cm) was used in all experiments.

Preparation of the CCM-WPC complex

A solution containing 0.50 g CCM (1.36 mmol) in 50 mL ethanol and a solution of 24.97 g WPC (1.36 mmol) in 1 L of water with NH_3 solution added dropwise to adjust the pH at 7.4 were prepared. The molar mass of β-lactoglobulin (18400 g/mol) was taken for the molar mass of WPC. The two solutions were mixed and stirred magnetically for 4 hours in dark condition, at room temperature. The resulting CCM and WPC (1:1 mole ratio) complex was dried using a Pilotech YC-018A spray dryer, at T_{in} of about 165 ^{o}C and T_{out} of around 49 ^{o}C, with ventilator frequency 58 Hz and solution flow rate 5 mL/min.

Samples preparation for AFM investigation

Curcumin was dispersed in ultrapure water, followed by homogenization with a magnetic stirrer at 500 rpm for 15 minutes. The CCM film adsorption was done in vertical plane on glass, 10 seconds, followed by natural drying at room temperature. For whey protein concentrate (WPC) and for the CCM-WPC complex, the process was similar.

Atomic Force Microscopy

AFM, JEOL JSPM 4210 model (Tokyo, Japan) was used to determine the NPs size and morphology of the layer of curcumin, whey protein concentrate and the CCM-WPC complex. The surface of the sample is scanned with a sharp tip (cantilever) that is brought as close as possible to its surface with optical technique so that AFM images are obtained by monitoring the change in amplitude of the cantilever oscillation during scanning. The measurements were performed in tapping mode (the most common mode of obtaining surface morphology) using a silicon nitride cantilever (NSC 15 Hard) purchased from MikroMasch, Sofia, Bulgaria, with a resonant frequency of 325 kHz and a force constant of 40 N/m.

The topographic, phase and amplitude images were obtained simultaneously at a scanning speed of about 1.2 Hz and their processing was performed with Win SPM2.0 Processing software, JEOL, Japan.

REFERENCES

1. B. Zheng; D.J. McClements; *Molecules*, **2020**, *25*, 2791.
2. V. Furlan; J. Konc; U. Bren; *Molecules*, **2018**, *23*, 3351.
3. S.S. Hettiarachchi; S.P. Dunuweera; A.N. Dunuweera; R.M.G. Rajapakse; *ACS Omega*, **2021**, *6*, 8246−8252.
4. M.U. Akbar; K. Rehman; K.M. Zia; M.I. Qadir; M.S.H. Akash; M. Ibrahim; *Crit. Rev. Eukaryot. Gene Expr.*, **2018**, *28*(1), 17–24.
5. M.L. Del Prado-Audelo; I.H. Caballero-Floran; J.A. Meza-Toledo; N. Mendoza-Munoz; M. Gonzalez-Torres; B. Floran; H. Cortes; G. Leyva-Gomez; *Biomolecules*, **2019**, *9*, 56.
6. L. Racz; M. Tomoaia-Cotisel; Cs.P. Racz; P. Bulieris; I. Grosu; S. Porav; A. Ciorita; X. Filip; F. Martin; G. Serban; I. Kacso; *Studia UBB Chemia*, **2021**, *66*(3), 209-224.
7. G.A. Paltinean; S. Riga; Gh. Tomoaia; A. Mocanu; M. Tomoaia-Cotisel; *Academy of Romanian Scientists Annals Series on Biological Sciences,* **2021**, *10*(2), 103-141.
8. K.I. Priyadarsini; *Molecules*, **2014**, *19*(12), 20091-20112.
9. B.H. Ali; H. Marrif; S.A. Noureldayem; A.O. Bakheit; G. Blunden; *Nat. Prod. Commun.*, **2006**, *1*(6), 509-521.
10. S. Solghi; Z. Emam-Djomeh; M. Fathi; F. Farahani; *J. Food Process Eng.*, **2020**, *43*(6), e13403.
11. V.S Ipar; A. Dsouza; P.V. Devarajan; *Eur. J. Drug Metab. Pharmacokinet.*, **2019**, *44*(4), 459-480.
12. M. Kharat; D.J. McClements; *J. Colloid Interface Sci.,* **2019**, *557*, 506–518.
13. A.D. Moghaddam; M. Mohammadian; A. Sharifan; S. Hadi; *J. Food Bioprocess Eng.*, **2019**, *2*(1), 55-60.
14. A.H. Sneharani; J.V. Karakkat; S.A. Singh; A.G.A. Rao; *J. Agric. Food Chem.*, **2010**, *58*(20), 11130–11139.

15. M. Li; Y. Ma; M. O. Ngadi; *Food Chem*., **2013**, *141*(2), 1504-1511.
16. P. Arya; N. Raghav; *J. Mol. Struct*., **2021**, *1228*, 129774.
17. H. Mashaqbeh; R. Obaidat; N. Al-Shar'l; *Polymers*, **2021**, *13*(23), 4073.
18. Cs.P. Racz; R.D. Pasca; S. Santa; I. Kacso; Gh. Tomoaia; A. Mocanu; O. Horovitz; M. Tomoaia-Cotisel; *Rev. Chim. (Bucharest*), **2011**, *62*(10), 992-997.
19. Cs.P. Racz; G. Borodi; M.M. Pop; I. Kacso; S. Santa; M. Tomoaia-Cotisel; *Acta. Crystallogr. B. Struct. Sci. Cryst. Eng. Mater*., **2012**, *68*(2), 164-170.
20. Cs.P. Racz; S. Santa; M. Tomoaia-Cotisel; G. Borodi; I. Kacso; A. Pirnau; I. Bratu; *J. Incl. Phenom. Macrocycl. Chem.,* **2013***, 76*(1), 193-199.
21. J. Burgain; R. El Zein; J. Scher; J. Petit; E.A. Norwood; G. Francius; C. Gaiani; *J. Food Eng*., **2016**, *178*, 39-46.
22. P.S. de P. Herrmann; C.M.P. Yoshida; A.J. Antunes; J.A. Marcondes; *Packag. Technol. Sci*., **2004**, *17*, 267–273.
23. P.X. Qi; C.I. Onwulata; *J. Dairy Sci*., **2011**, *94*(5), 2231–2244.
24. G.T. D. Sousa; F.S. Lira; J.C. Rosa; E.P. de Oliveira; L.M. Oyama; R.V. Santos; G.D. Pimentel; *Lipids Health Dis*., **2012**, *11*, 67.
25. U.S. Dairy Export Council; *Reference Manual for U.S. Whey and Lactose Products*, edited by V. Lagrange; U.S. Dairy Export Council, Arlington, USA, **2003**, pp. 1-226.
26. G.K. Gbassi; F.S. Yolou; S.O. Sarr; P.G. Atheba; C.N. Amin; M. Ake*; Int. J. Biol. Chem. Sci.,* **2012**, *6*(4), 1828-1837.
27. S. Patel; *J. Funct. Foods*, **2015**, *19*, 308–319.
28. S. Minj; S. Anand; *Dairy*, **2020**, *1*, 233–258.
29. A.R. da Conceicao; K.A. Dias; S.M.S. Pereira; L.C. Saraiva; L.A. Oliveira; E.C. Gomes de Souza; R.V. Goncalves; S.L.P. da Matta; A.J. Natali; H.S.D. Martino; C.M. Della Lucia; *Br. J. Nutr*., **2022**, *127*, 526–539.
30. A. Nayak; C. Genot; A. Meynier; A. Dorlando; I. Capron; *LWT,* **2022,** *153*, 112421.
31. Y. Wen; Z. Xu, Y. Liu; H. Corke; Z. Sui; *Compr. Rev. Food Sci. Food. Saf*., **2020**, 1–24.
32. R.D. Pasca; Gh. Tomoaia; A. Mocanu; I. Petean; A.G. Paltinean; O. Soritau; M. Tomoaia-Cotisel; *Studia UBB Chemia*, **2015**, *60*(3), 257-264.
33. Gh. Tomoaia; O. Soritau; M. Tomoaia-Cotisel; L.B. Pop; A. Pop; A. Mocanu; O. Horovitz; L.D. Bobos; *Powder Technol*., **2013**, *238*, 99-107.
34. Gh. Tomoaia; M. Tomoaia-Cotisel; L.B. Pop; A. Pop; O. Horovitz; A. Mocanu; N. Jumate; L.D. Bobos; *Rev. Roum. Chim*., **2011**, *56*(10-11), 1039-1046.
35. A. Mocanu; I. Cernica; Gh. Tomoaia; L.D. Bobos; O. Horovitz; M. Tomoaia-Cotisel; *Colloid Surf. A*, **2009**, *338*(1-3), 93-101.
36. Gh. Tomoaia; O. Horovitz; A. Mocanu; A. Nita; A. Avram; Cs.P. Racz; O. Soritau; M. Cenariu; M. Tomoaia-Cotisel; *Colloids Surf. B*, **2015**, *135*, 726-734.

37. A. Mocanu; O. Cadar; P.T. Frangopol; I. Petean; Gh. Tomoaia; G.A. Paltinean; Cs.P. Racz; O. Horovitz; M. Tomoaia-Cotisel; *R. Soc. Open Sci.*, **2021**, *8*(1), 201785.

38. C. Garbo; J. Locs; M. D'Este; G. Demazeau; A. Mocanu; C. Roman; O. Horovitz; M. Tomoaia-Cotisel; *Int. J. Nanomed.*, **2020**, *15*, 1037-1058.

39. D. Oltean-Dan; G.B. Dogaru; M. Tomoaia-Cotisel; D. Apostu; A. Mester; H.R. C. Benea; M.G. Paiusan; E.M. Jianu; A. Mocanu; R. Balint; C.O. Popa; C. Berce; G.I. Bodizs; A.M. Toader; Gh. Tomoaia; *Int. J. Nanomed.*, **2019**, *14*, 5799-5816.

40. D. Oltean-Dan; G.B. Dogaru; E.M. Jianu; S. Riga; M. Tomoaia-Cotisel; A. Mocanu; L. Barbu-Tudoran; Gh. Tomoaia; *Micromachines*, **2021**, *12*(11), 1352.

41. A. Mocanu; G. Furtos; S. Rapuntean; O. Horovitz; F. Chirila; C. Garbo; A. Danisteanu; G. Rapuntean; C. Prejmerean; M. Tomoaia-Cotisel; *Appl. Surf. Sci.*, **2014**, *298*, 225-235.

42. C. Garbo; M. Sindilaru; A. Carlea; Gh. Tomoaia; V. Almasan; I. Petean; A. Mocanu; O. Horovitz; M. Tomoaia-Cotisel; *Part. Sci. Technol.*, **2017**, *35*(1), 29-37.

43. G. Furtos; M. Tomoaia-Cotisel; C. Garbo; M. Senila; N. Jumate; I. Vida-Simiti; C. Prejmerean; *Part. Sci. Technol.*, **2013**, *31*(4), 392-398.

44. G.A. Hosu-Prack; I. Petean; G. Arghir; L.D. Bobos; I. Iurcut; M. Tomoaia-Cotisel; *Carpathian J. Earth Environ. Sci.*, **2013**, *8*(4), 75-82.

45. G.A. Paltinean; I. Petean; G. Arghir; D.F. Muntean; L.D. Bobos; M. Tomoaia-Cotisel; *Partic. Sci. Technol.*, **2016**, *34*(5), 580-585.

46. M. Tomoaia-Cotisel; A. Tomoaia-Cotisel; T. Yupsanis; Gh. Tomoaia; I. Balea; A. Mocanu; Cs.P. Racz; *Rev. Roum. Chim.*, **2006**, *51*(12),1181-1185.

47. O. Horovitz; Gh. Tomoaia; A. Mocanu; T. Yupsanis; M. Tomoaia-Cotisel; *Gold Bull.*, **2007**, *40*(3), 213-218.

48. O. Horovitz; A. Mocanu; Gh. Tomoaia; L.D. Bobos; D. Dubert; I. Daian; T. Yupsanis; M. Tomoaia-Cotisel; *Studia UBB Chemia*, **2007**, *52*(1), 97-108.

49. O. Horovitz; A. Mocanu; Gh. Tomoaia; M. Crisan; L.D. Bobos; Cs.P. Racz; M. Tomoaia-Cotisel; *Studia UBB Chemia*, **2007**, *52*(3), 53-71.

50. M. Tomoaia-Cotisel; A. Mocanu; *Rev. Chim. (Bucharest)*, **2008**, *59*(11), 1230-1233.

51. P.T. Frangopol; D.A. Cadenhead; M. Tomoaia-Cotisel; A. Mocanu; *Studia UBB Chemia*, **2009**, *54*(1), 23-35.

52. I. Balea; M. Tomoaia-Cotisel; O. Horovitz; Gh. Tomoaia; A. Mocanu; *Studia UBB Chemia*, **2009**, *54*(1), 151-163.

53. Gh. Tomoaia; C. Borzan; M. Crisan; A. Mocanu; O. Horovitz; L.D. Bobos; M. Tomoaia-Cotisel; *Rev. Roum. Chim.*, **2009**, *54*(5), 363-372.

54. O. Monfort; L.C. Pop; S. Sfaelou; T. Plecenik; T. Roch; V. Dracopoulos; E. Stathatos; G. Plesch; P. Lianos; *Chem. Eng. J.*, **2016,** *286,* 91-97.

55. M. Tomoaia-Cotisel; D.V. Pop-Toader; U.V. Zdrenghea; Gh. Tomoaia; O. Horovitz; A. Mocanu; *Studia UBB Chemia.*, **2009**, *54*(4), 285-296.

56. U.V. Zdrenghea; Gh. Tomoaia; D.V. Pop-Toader; A. Mocanu; O. Horovitz; M. Tomoaia-Cotisel; *Comb. Chem. High Throughput Screen.*, **2011**, *14*(4), 237-247.

57. P.T. Frangopol; D.A. Cadenhead; Gh. Tomoaia; A. Mocanu; M. Tomoaia-Cotisel; *Rev. Roum. Chim.*, **2015**, *60*(2-3), 265-273.

58. A. Mocanu; P.J. Quinn; C. Nicula; S. Riga; Gh. Tomoaia; C.A. Bardas; M. Tomoaia-Cotisel; *Rev. Roum. Chim.*, **2021**, *66*(10-11), 855-869.

59. Gh. Tomoaia; M. Tomoaia-Cotisel; A. Mocanu; O. Horovitz; L.D. Bobos; M. Crisan; I. Petean; *J. Optoelectron. Adv. Mater.*, **2008**, *10*(4), 961-964.

60. A.G. Hosu-Prack; I. Petean; G. Arghir; L.D. Bobos; M. Tomoaia Cotisel; *Carpathian J. Earth Environ. Sci.,* **2016**, *11*(2), 539-546.

61. M. Mohammadian; M. Salami; F. Alavi; S. Momen; Z. Emam-Djomeh; A.A. Moosavi-Movahedi; *Food Biophys.*, **2019**, *14*, 425–436.

62. M. Mohammadian; A.D. Moghaddam; A. Sharifan; P. Dabaghi; S. Hadi*; J. Iran Chem. Soc.*, **2020**, *17*, 2481–2492.